Phase diagram and bulk thermodynamical quantities in the Nambu–Jona-Lasinio model at finite temperature and density

T. M. Schwarz, S. P. Klevansky, and G. Papp*
Institut für Theoretische Physik, Universität Heidelberg, Philosophenweg 19, D-69120, Heidelberg, Germany
(Received 11 June 1999; published 1 October 1999)

We reexamine the recent instanton motivated studies of Alford, Rajagopal, and Wilczek, and Berges and Rajagopal in the framework of the standard SU(2) Nambu–Jona-Lasinio (NJL) model. The chiral phase diagram is calculated in the temperature-density plane, and the pressure is evaluated as the function of the quark density. Obtaining simple approximate relations describing the T-μ and T-p_F phase transition lines, we find that the results of the instanton based model and that of the NJL model are identical. The diquark transition line is also given. [S0556-2813(99)06210-X]

PACS number(s): 11.30.Rd, 12.38.Mh, 11.10.Wx

I. INTRODUCTION

Recent studies by several authors using an effective four-fermionic interaction between quarks [1–3] or direct instanton approach [4] have rekindled interest in the two flavor QCD phase transitions. In particular, Alford, Rajagopal, and Wilczek [1] have studied the pressure density and gap parameter using a fermionic Lagrangian with an instanton motivated four-point interaction. At zero temperature, these authors found negative pressure for a certain range of the Fermi momentum $p_{\rm F}$ and showed the solutions of the gap equation as a function of $p_{\rm F}$. Berges and Rajagopal [2] extended this work and have calculated the phase diagram of a strongly interacting matter as a function of temperature and baryon number density in the same model.

The question that we raise and examine in this paper is whether or not these results are fundamentally different from those obtained via the standard well-known Nambu–Jona-Lasinio (NJL) model [5–10], at least with regard to chiral symmetry breaking. Quantities such as the gap parameter, pressure density, and other thermodynamical quantities have been extensively studied in this model over the last decade [6,8,11,12], and even to a level of sophistication that goes beyond the standard mean field treatments [11,12]. However, the results have usually been presented as a function of the chemical potential, and not as of the Fermi momentum $p_{\rm F}$ or density, as the authors of [1,2] have done, and hence the connection between their results and those of the NJL model are not obvious. Thus, in order to make a systematic comparison, we have to reevaluate the gap, pressure, and phase diagram in these variables. In Sec. II we derive a simple analytical approximate expression for the phase boundary that is independent of the parameters of the NJL model. In Sec. III, we examine the pressure as a function of the density and calculate the complete chiral phase diagram numerically from Maxwell constructions. We compare our results with that of Ref. [2]. In Sec. IV, we write down the form of the gap equation for a superconducting diquark transition, and thus the line of points in the T-μ plane. This is evaluated numerically. We summarize and conclude in Sec. V.

II. PHASE BOUNDARY CURVE—AN ANALYTIC EXPRESSION

We commence by deriving an approximate analytic expression for the phase boundary curve. Our starting point is the gap equation for the dynamically generated up and $down$ quark mass m that is derived from the SU(2) chirally symmetric Lagrangian

$$\mathcal{L}_{\rm NJL}=\bar{\psi}i\partial\!\!\!/\psi+G[(\bar{\psi}\psi)^2+(\bar{\psi}i\gamma_5\vec{\tau}\psi)^2], \tag{1}$$

with G a dimensionful coupling and ψ quark spinors for u and d quarks. At nonzero temperature and chemical potential, the mean-field self-energy or gap equation reads [6]

$$\Sigma^*=m=4GN_cN_fm\int\frac{d^3p}{(2\pi)^3}\frac{1}{E_p}[1-f^+(\vec{p},\mu)-f^-(\vec{p},\mu)], \tag{2}$$

with the Fermi distribution functions $f_p^{\pm}\equiv 1/[e^{\beta(E_p\pm\mu)}+1]=f^{\pm}(\vec{p},\mu)$. The gap equation is easily seen to minimize the thermodynamical potential [6,15]

$$\Omega(m)=\frac{m^2}{4G}-\gamma\int\frac{d^3p}{(2\pi)^3}E_p-\gamma T\int\frac{d^3p}{(2\pi)^3}\times\ln[1+e^{-\beta(E_p+\mu)}][1+e^{-\beta(E_p-\mu)}], \tag{3}$$

where $E_p^2=p^2+m^2$, $\beta=1/T$ and $\gamma=2N_cN_f$ is the degeneracy factor. The condensate is related to m via $m=-2G\langle\bar{\psi}\psi\rangle$. The three momentum integrals are understood to be regulated by a cutoff Λ, and a standard set of parameters; $\Lambda=0.65$ GeV and $G=5.01$ GeV^{-2} are used to fix the values of $f_\pi=93$ MeV and the condensate density per flavor, $\langle\bar{u}u\rangle=\langle\bar{d}d\rangle=(-250\ \text{MeV})^3$.

Let us examine first the $T=0$ limit of Eq. (2). The gap equation for the nontrivial solution is

*On leave from HAS Research Group for Theoretical Physics, Eötvös University, Budapest, Hungary.

$$\frac{\pi^2}{2GN_cN_f}=\int_{p_F}^{\Lambda} dp\,\frac{p^2}{\sqrt{p^2+m^2}} \tag{4}$$

in terms of the Fermi momentum p_F. p_F is a decreasing function of the constituent mass taking its maximum value p_c at the chiral phase transition $m\to 0$:[1]

$$p_c=\Lambda\sqrt{1-\frac{\pi^2}{G\Lambda^2N_cN_f}}. \tag{5}$$

Using the numerical values of G and Λ given above and fixing $N_c=3$, $N_f=2$ leads to the numerical value $p_c=0.307$ GeV. We use this relation to eliminate Λ^2 in favor of p_c^2. Now, in order to determine the phase transition line, we start with the gap equation (2) and divide $m\neq 0$ out. The critical values of the temperature and chemical potential that lie on the phase transition boundary are determined through the vanishing chiral condensate and hence $m\to 0$. Performing the usual substitution $u=\beta(p\pm\mu)$ as appropriate, and evaluating the integral on the right hand side, one finds

$$\mu^2=p_c^2-\frac{\pi^2T^2}{3}. \tag{6}$$

This equation defines the chiral phase transition curve in the T-μ plane, and in this form contains no explicit model dependence on G and Λ. We would, however, prefer to display the phase transition line as a function of temperature and quark density. To do so, we express the density through the Fermi momentum, p_F at zero temperature,

$$n=\frac{2N_cN_f}{6\pi^2}p_F^3. \tag{7}$$

At finite temperature, the quark density n is given as

$$n=2N_cN_f\int\frac{d^3p}{(2\pi)^3}[f_p^- - f_p^+]. \tag{8}$$

The cube root of the density defines n_3 as $n^{1/3}=cn_3$, where $c=2/\pi^2$, and n_3 is evaluated to be

$$n_3=\left[3\sinh\left(\frac{\mu}{T}\right)\cdot\int dp\frac{p^2}{\cosh(\mu/T)+\cosh(E_p/T)}\right]^{1/3}. \tag{9}$$

Using this transformation, we can display all quantities as functions of n_3 (or density) and not of the chemical potential μ any more. One can take a set of T and μ and calculate, for example, $m(T,\mu)$ and $n_3(T,\mu)$. The result obtained can be seen in Fig. 1 where for fixed T, $T=0$ the mass m is plotted

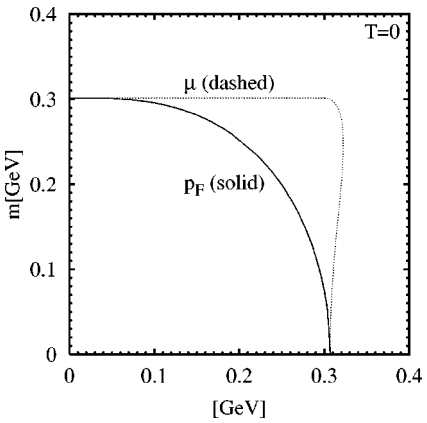

FIG. 1. The gap parameter m shown both as a function of μ (solid curve) and p_F (dotted line) at $T=0$.

as a function of p_F (solid line) and of μ (dashed line) for comparison. We note that the behavior found is qualitatively the same as that in [1]. At the chiral phase transition point, $m\to 0$ and $n_3\to n_{3,c}$ with

$$n_{3,c}^3=\mu(\mu^2+\pi^2T^2). \tag{10}$$

This expression can be used to eliminate μ from Eq. (6) and the chiral phase transition curve in the T-n_3 plane is determined from the simple analytical expression

$$\frac{4\pi^6}{27}T^6-\pi^2p_c^4T^2+(n_{3,c}^6-p_c^6)=0. \tag{11}$$

The solution of this third order equation in T^2, defining the critical temperature T_c at which the phase transition occurs for a given ratio $\rho=n_{3,c}/p_c$ can be written as

$$T_c(\rho)=\frac{\sqrt{3}p_c}{\pi}\sqrt{\cos\left(\frac{1}{3}\kappa\rho\right)}\leqslant\frac{\sqrt{3}}{\pi}p_c, \tag{12}$$

with

$$\kappa=\begin{cases}\tan^{-1}\sqrt{[\rho^6-1]^{-2}-1} & \rho\leqslant 1,\\ \pi+\tan^{-1}\sqrt{[\rho^2-1]^{-2}-1} & 1\leqslant\rho\leqslant 2^{1/6}.\end{cases} \tag{13}$$

The trivial solution to the gap equation is the only solution if the temperature exceeds the maximum value of the critical temperature on the transition curve,

$$T_m=\frac{\sqrt{3}p_c}{\pi}\simeq 0.169\ \text{GeV}, \tag{14}$$

or if $n_{3,c}/p_c\geqslant 2^{1/6}$. One can now recast the solution for $n_{3,c}$ in terms of T_m yielding a parameter-free normalized relation:

$$\left(\frac{n_{3,c}}{p_c}\right)^3=\left[2\left(\left(\frac{T}{T_m}\right)^2+1\right)\right]\sqrt{1-\left(\frac{T}{T_m}\right)^2}. \tag{15}$$

[1]Here we assume a second order transition where the smooth vanishing of the order parameter signals the transition. However, for small temperatures the phase transition is of first order with a jump in the order parameter. Nevertheless, the approximation made here qualitatively gives the proper answer (cf. Fig. 2).

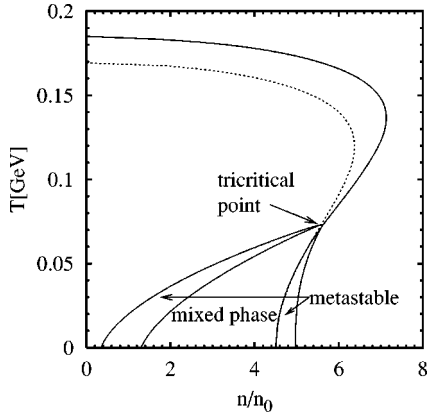

FIG. 2. The phase diagram calculated from the approximate analytical form (11) (dashed line) and as determined numerically (solid lines) as a function of the quark density n, scaled by normal nuclear matter density $n_0=0.17\ \mathrm{fm}^{-3}$.

We illustrate this relation in a more usual way in Fig. 2, plotting the critical value of the temperature as a function of the quark density divided by normal nuclear matter density $n_0=0.17\ \mathrm{fm}^{-3}$.

III. PHASE TRANSITION CURVE VIA MAXWELL CONSTRUCTION

We return now to the thermodynamical quantities. From Eq. (3) for $\Omega(m)$, it follows that the pressure density is given as

$$p=-\Omega=\frac{\gamma}{\beta}\int\frac{d^3p}{(2\pi)^3}\ln[(1+e^{-\beta(E_p+\mu)})(1+e^{-\beta(E_p-\mu)})]+\gamma\int\frac{d^3p}{(2\pi)^3}E_p-\frac{m^2}{4G}. \tag{16}$$

The energy density is found to be

$$\epsilon=\gamma\int\frac{d^3p}{(2\pi)^3}E_p[f_p^-+f_p^+]-\gamma\int\frac{d^3p}{(2\pi)^3}E_p+\frac{m^2}{4G}. \tag{17}$$

In the limit $T\to 0,\mu\to 0$, one has

$$\epsilon_{\mathrm{vac}}=\epsilon_{T\to 0,\mu\to 0}=\frac{m^{*2}}{4G}-\frac{N_cN_f}{\pi^2}\int_0^\Lambda dpp^2\sqrt{p^2+m^{*2}}, \tag{18}$$

where $m^*=m(T=0,\mu=0)$, while an analogous calculation for the pressure density p at $T\to 0$, $\mu\to 0$ yields

$$p_{\mathrm{vac}}=-\epsilon_{\mathrm{vac}}. \tag{19}$$

p_{vac} and ϵ_{vac} are independent of temperature and chemical potential and their value is (up to the sign) the same. For our choice of parameters, $\epsilon_{\mathrm{vac}}=-(407\ \mathrm{MeV})^4$. Measuring the pressure and energy densities relative to their vacuum values, we have

$$\epsilon_{\mathrm{phys}}=\epsilon-\epsilon_{\mathrm{vac}}, \tag{20}$$

$$p_{\mathrm{phys}}=p+\epsilon_{\mathrm{vac}}. \tag{21}$$

In Fig. 3, we plot the pressure density as a function of n_3 for a range of temperatures. Note that at $T=0$, p becomes *negative* and displays a cusplike structure. This is brought about by the fact that the two solutions for the gap equation enter into the pressure density on the different arms of the pressure: the rising curve is brought about by the $m=0$ solution, while the solution that goes down has a value of $m\neq 0$. Note that this situation is similar to that observed in Ref. [1].

The phase transition curve can now be calculated using a more standard but numerical treatment and compared to the approximate (second order) curve shown as the dashed line in Fig. 2. The difference between these two curves lies in the fact that the analytic one is calculated with $\Lambda\to\infty$, while the numerical curve has Λ finite. It is worth noting that the truncation of the NJL model to zero modes [13] shows a similar behavior to the one observed in the full model, however, lacking the unstable backbending of the phase curve at high temperatures. Plotting the pressure instead as a function of volume allows one to perform Maxwell constructions and obtain the full information of the phase diagram, including the metastable region. The results of this calculation are shown in Fig. 4 as a function of $n^{1/3}$ as the solid curves. Also shown (dashed curves) are the calculations of Ref. [2]. We note that the phase transition curve for the chiral transition are qualitatively identical. The main difference between these curves lies in the observation that the mixed phase

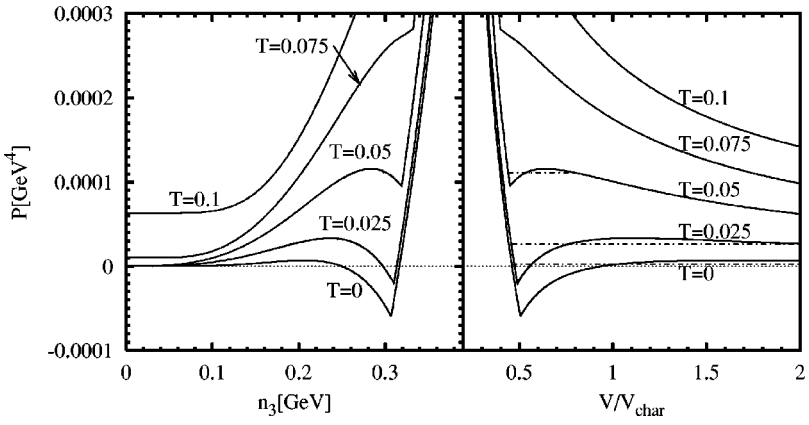

FIG. 3. Pressure shown as a function of $n_3=(2/\pi^2)n$ (left side) and as a function of the volume, normalized by a characteristic volume.

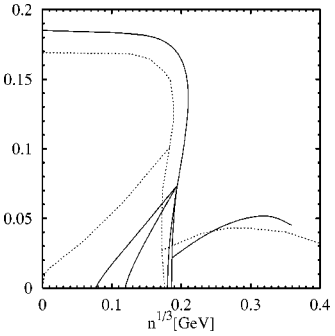

FIG. 4. Direct comparison of the NJL phase diagram (solid lines) shown as a function of $n^{1/3}$, with that of [2] (dashed lines). The lines to the right of $n^{1/3}\sim 0.19$ are the superconducting transition lines.

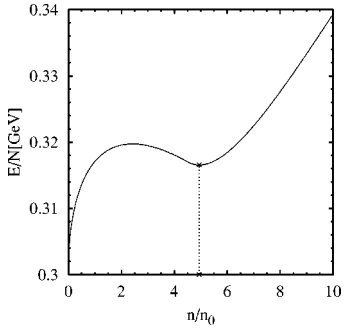

FIG. 5. The energy per quark shown as a function of n/n_0. The minimum occurs at approximately $n\simeq 5n_0$ and not at $n=3n_0$.

given by Ref. [2] already starts at $n=0$, similarly to the truncated NJL calculation [13]. The equivalence of these models is perhaps not simply apparent when one examines the Lagrangians. However, the thermodynamical potential of Ref. [2] is precisely that of Eq. (3) in the absence of the diquark condensate. Thus the differences observed in Fig. 4 can only be attributed to the use of slightly different parameters; in addition the different method of implementing regularization—in the NJL model here, a ''hard'' cutoff Λ is employed, and in the approximate expression for the phase curve, is also taken as $\Lambda\rightarrow\infty$, while the authors of [1,2] use a soft form factor $F(p)=\Lambda^2/(p^2+\Lambda^2)$ to regulate their momentum integrals. The physics however cannot and does not depend on this and the qualitative results remain unchanged.

Limitations and difficulties of this model in describing thermodynamical quantities are well known [12,14]. We illustrate one problem in showing the energy per quark plotted at $T=0$ as a function of the density in Fig. 5. This quantity does not posses a minimum at normal nuclear matter density as expected, in apposition to recent linear sigma model calculations [16].

IV. DIQUARK CONDENSATE TRANSITION LINE

The thermodynamic potential for three colors[2] $\Omega(m)$ given in Eq. (3) corresponds precisely to the $\Delta=0$ limit of the function $\Omega(m,\Delta)$ [2]:

$$\Omega(m,\Delta)=\frac{m^2}{4G}+\frac{\Delta^2}{4G_1}-2N_f\int\frac{d^3p}{(2\pi)^3}\{(N_c-2)\times[E_p+T\ln(1+e^{-\beta(E_p-\mu)})(1+e^{-\beta(E_p+\mu)})]+\sqrt{\xi_+^2+\Delta^2}+s\sqrt{\xi_-^2+\Delta^2}+2T\times\ln(1+e^{-\beta\sqrt{\xi_+^2+\Delta^2}})\times(1+e^{-\beta s\sqrt{\xi_-^2+\Delta^2}})\}, \tag{22}$$

where $\xi_\pm=E_p\pm\mu$, and Δ is the color superconducting condensate in the diquark channel. s is a sign function, and $s=\pm 1$ for $E_p>\mu$ or $E_p<\mu$. Here the expression from [2] has been modified to remove the form factor—instead a 3D cutoff $|\vec{p}|<\Lambda$ as is usual in the NJL model and which was used in the previous section is to be understood. G_1 is a new coupling strength mediating a four-fermion interaction that is attractive in the diquark channel. The form for $\Omega(m)=\Omega(m,0)$ from Eq. (3) thus indicates that the models are the same, and the same gap equation for the chiral transition is retained. For the superconducting sector, the gap obtained by differentiating $\Omega(0,\Delta)$ with respect to Δ is

$$\frac{1}{2G_1}=2N_F\int\frac{d^3p}{(2\pi)^3}\left\{\frac{1}{\sqrt{\xi_+^2+\Delta^2}}\tanh\frac{\beta}{2}\sqrt{\xi_+^2+\Delta^2}+\frac{1}{\sqrt{\xi_-^2+\Delta^2}}\tanh\frac{\beta}{2}\sqrt{\xi_-^2+\Delta^2}\right\}. \tag{23}$$

This expression is a relativistic generalization of the superconducting gap equation for electron pairs [17] in which the quasiparticle energies $\sqrt{\xi_-^2+\Delta^2}$ and $\sqrt{\xi_+^2+\Delta^2}$ relative to the Fermi surface are introduced. Note that at $T=0$, one recovers the result of [1] for $\mu\neq 0$, assuming that the form factor of these authors is set to one. The phase transition line in the T-μ or T-n_3 planes can now be obtained quite simply. Assuming that the superconducting phase transition can only occur in the region where chiral symmetry is restored, we may set $E=p$. Furthermore we assume the transition to be of second order, driven by the condition $\Delta\rightarrow 0$. Thus the T-μ critical curve satisfies

$$\frac{\pi^2}{2N_fG_1}=\int_0^\Lambda dpp^2\frac{1}{p+\mu}\tanh\frac{1}{2}\beta(p+\mu)+\int_\mu^\Lambda dpp^2\frac{1}{p-\mu}\tanh\frac{1}{2}\beta(p-\mu)+\int_0^\mu dpp^2\frac{1}{\mu-p}\tanh\frac{1}{2}\beta(\mu-p), \tag{24}$$

which, with obvious changes of variables, reduces to

[2]For two colors a massless pionic diquark may form.

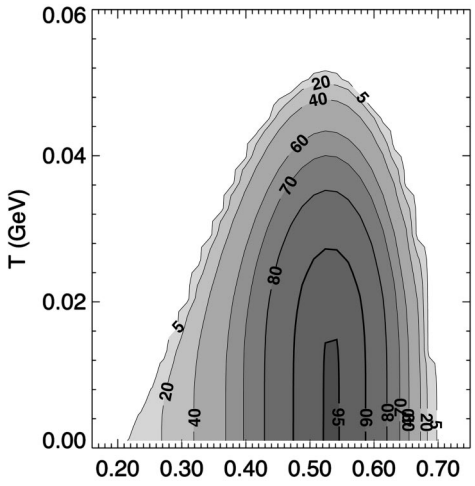

FIG. 6. The diquark gap parameter Δ shown as a function of μ and T. The contour values are given in MeV.

$$\frac{\pi^2}{2N_f G_1} = \int_0^{\Lambda+\mu} d\xi \left(\xi - 2\mu + \frac{\mu^2}{\xi} \right) \tanh \frac{1}{2}\beta\xi + \int_0^{\Lambda-\mu} d\xi \left(\xi + 2\mu + \frac{\mu^2}{\xi} \right) \tanh \frac{1}{2}\beta\xi. \quad (25)$$

Unlike the case for electron pairing, in which $\mu \gg \omega_D$, with ω_D the Debye frequency, we cannot regard the logarithmic term as being leading, and it is not possible to obtain a simple analytic expression for the right-hand side of Eq. (25). We thus solve Eq. (25) numerically for the critical line. Clearly this depends on the choice of the strength G_1 and is a sensitive function thereof. Arbitrarily demanding that $T_c = 40$ MeV at $\mu = 0.4$ GeV close to the values of Ref. [2] sets $G_1 = 3.10861$ GeV^{-2}, or $G_1\Lambda^2 = 1.31$. The resulting curve is indicated by the dotted line in Fig. 4. As can be seen, the qualitative behavior of the model of Ref. [2] is confirmed. We found a somewhat lower gap, Δ being ~ 35 MeV at the chiral transition point and zero temperature increasing up to ~ 95 MeV at and $\mu = 0.53$ GeV and zero temperature. The general behavior of the gap parameter as a function of the chemical potential and temperature is given in Fig. 6.

Finally, we comment that although the diquark phase transition line was investigated here under the expectation that chiral symmetry is restored, this is not necessarily the case: in principle, the diquark phase transition line can extend into the region in which chiral symmetry is broken, i.e., where $\langle \bar{\psi}\psi \rangle \neq 0$ or $m \neq 0$. In practice, this turns out to be a function of the parameters chosen. If the diquark phase transition line enters into the region of chiral symmetry breaking at a temperature larger than the tricritical temperature, the dependence of $m(T,\mu)$ that enters into Eq. (23) is continuous, and a solution to this equation can be found. For our choice of G_1, however, the diquark transition line would enter into the region where a first order phase transition takes place. Thus $m(T,\mu)$ is discontinuous, and no physically accessible solution to this equation can be found. The situation

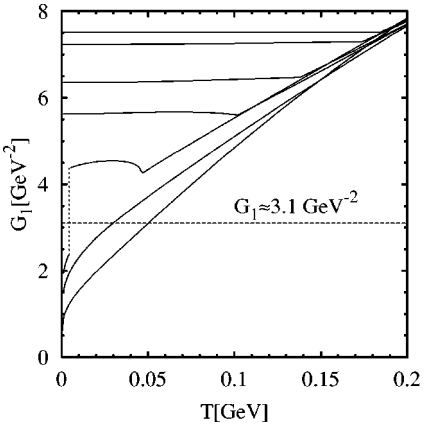

FIG. 7. The functional dependence of G_1 as calculated from Eq. (23) is plotted as a function of the temperature for different values of the chemical potential. The curves, taken from the uppermost one, correspond to the values of $\mu = 0$, 0.1, 0.2, 0.25, 0.3, 0.35, and 0.5 GeV.

is illustrated in Fig. 7, in which Eq. (23) is inverted and solved for G_1 and the functional dependence, as well as the numerical parameter value 3.1 GeV^{-2}, are plotted as a function of temperature for several values of μ. One sees from this figure that the line $G_1 = 3.1$ GeV^{-2} cannot intersect the curve $\mu = 0.3$ GeV, for example, which lies in the broken phase, and therefore there is no physically attainable solution. Note however that by adjusting the value of the constant G_1 to a somewhat smaller value could admit a solution within this region.

V. CONCLUSIONS

In analyzing the chiral phase transition in the NJL model at finite temperature and density, we find the same behavior for the chiral and diquark phases as that reported in Refs. [1,2], which use an instanton motivated interaction that is also four point in nature. That this must occur can be seen directly from the explicit form of the thermodynamical potential that is well known in our case [6,15], and which is obtained from [2] on setting the form factor to one and introducing a 3D cutoff Λ. In addition, we are easily able to give an approximate analytic form for the chiral phase curve in the T-μ and T-n_3 planes that is independent of the model parameters. We have examined the extended form of the thermodynamic potential that makes provisions for a diquark condensate and obtained the appropriate critical line in the NJL model. Our qualitative results conform with those of [2]. In addition, we find evidence for the appearance of a diquark condensate also within the region where chiral symmetry is not restored, but this is strongly parameter dependent.

ACKNOWLEDGMENTS

One of us, G.P., thanks Michael Buballa and Maciej A. Nowak for the discussions and comments. This work has been supported by the German Ministry for Education and Research (BMBF) under Contract No. 06 HD 856, and by Grant No. OTKA-F019689.

[1] M. Alford, K. Rajagopal, and F. Wilczek, Phys. Lett. B **422**, 247 (1998).
[2] J. Berges and K. Rajagopal, Nucl. Phys. **B538**, 215 (1999); G. W. Carter and D. Diakonov, Nucl. Phys. **A642**, 78 (1998); nucl-th/9908019.
[3] E. Shuryak, hep-ph/9903297.
[4] R. Rapp, T. Schäfer, E. Shuryak, and M. Velkovsky, Phys. Rev. Lett. **81**, 53 (1998); hep-ph/9904353.
[5] Y. Nambu and G. Jona-Lasinio, Phys. Rev. **122**, 345 (1961); **124**, 246 (1961).
[6] S. P. Klevansky, Rev. Mod. Phys. **64**, 649 (1992).
[7] U. Vogl and W. Weise, Prog. Part. Nucl. Phys. **27**, 91 (1991).
[8] T. Hatsuda and T. Kunihiro, Phys. Rep. **247**, 241 (1994).
[9] C. V. Christov *et al.*, Prog. Part. Nucl. Phys. **37**, 91 (1996).
[10] R. Alkofer, H. Reinhardt, and H. Weigel, Phys. Rep. **265**, 139 (1996).
[11] J. Hüfner, S. P. Klevansky, and P. Zhuang, Ann. Phys. (N.Y.) **234**, 225 (1994).
[12] P. Zhuang, J. Hüfner, and S. P. Klevansky, Nucl. Phys. **A576**, 525 (1994).
[13] R. A. Janik, M. A. Nowak, G. Rapp, and I. Zahed, Nucl. Phys. **A642**, 191 (1998).
[14] M. Buballa, Nucl. Phys. **A611**, 393 (1996).
[15] M. Asakawa and K. Yazaki, Nucl. Phys. **A504**, 668 (1989).
[16] J. Meyer and H.-J. Pirner (private communication); nucl-th/9908019.
[17] A. L. Fetter and J. D. Walecka, *Quantum Theory of Many-Particle Systems* (McGraw-Hill, New York, 1971).